RESEARCH ARTICLE

Removal of Cadmium from Aqueous Solutions using Nickel Hydroxide/Reduced Graphene Oxide Composite: Response Surface Methodology Optimization and Nonlinear Isotherm Modeling

Elif Öztürk Er[1,2*] iD

[1]İstanbul Technical University, Department of Chemical Engineering, 34469 İstanbul, Türkiye
[2]İstanbul Technical University, Nanotechnology Application and Research Center, 34469 İstanbul, Türkiye

Abstract: Removal of Cd(II) ions from aqueous solutions was investigated using a nickel hydroxide/reduced graphene oxide composite as the adsorbent material. Influential parameters of the batch adsorption process were optimized using the Box-Behnken design, which enabled a systematic evaluation of the effects of various factors. An analysis of variance was performed to develop a quadratic regression model for predicting the percentage of Cd(II) removal. The optimal conditions for achieving maximum removal efficiency were identified as an adsorbent dosage of 60 mg, a pH of 8.0, and a mixing period of 40 minutes. Isotherm analysis was conducted using nonlinear regression, with the sum of squared errors serving as the error function. The results indicated that the Langmuir model provided a better fit to the experimental data compared to the Freundlich model, as evidenced by higher determination coefficients (0.9684) and lower error values. This suggested that the adsorption process is characterized by a monolayer adsorption mechanism on a homogeneous surface. The maximum adsorption capacity was found to be 218 mg/g, indicating the effectiveness of the nickel hydroxide/reduced graphene oxide composite in removing Cd(II) ions from solution.

Keywords: Cadmium, Metal oxide, Graphene Oxide, Adsorption Isotherms, Nonlinear Regression.

1. INTRODUCTION

Release of heavy metals into aquatic environments has become a significant environmental concern due to their persistent and toxic nature. Unlike organic pollutants, heavy metals do not degrade and can accumulate in ecosystems, posing long-term threats to both the environment and human health. Cadmium (Cd), a particularly hazardous heavy metal, is extensively used in industries such as battery manufacturing, electroplating, textile processing, pesticides, dyes and plastic production. The ongoing industrial activity involving Cd-containing products significantly impacts the environment, leading to increased Cd levels and high exposure risks to human health (Charkiewicz et al., 2023).

In recent years, extensive research has focused on the biological effects of Cd, which is classified as a toxic and carcinogenic substance, with the potential to stimulate various harmful biological processes. Cd tends to accumulate predominantly in the kidneys and liver, each storing about 30%, while the rest is dispersed across other organs. This accumulation is concerning due to its exceptionally long biological half-life, which can extend from 10 to 30 years (Peana et al., 2023). The accumulation of Cd in various tissues causes the disruption of key cellular processes like proliferation and differentiation, and triggers oxidative stress by

promoting the formation of reactive oxygen species. Prolonged exposure to Cd causes long-term damage in the body, weakens bones, contributes to cardiovascular problems and increases the risks of cancers in the lungs, prostate and other organs (Hayat et al., 2019) (Gulisano et al., 2009). Because of its toxic effects, the removal of cadmium from environmental sources is critical to prevent contamination of water bodies.

A range of treatment technologies such as ion-exchange processes, electrochemical methods and chemical precipitation have been employed for the removal of heavy metals from water bodies (Goyal et al., 2021; Hosseini et al., 2020; Kim et al., 2024; Pohl, 2020; Sun et al., 2020; Zhang & Duan, 2020). However, adsorption has emerged as a favored approach due to its economic viability, ease of operation, and ability to effectively handle trace amounts of metal contaminants. The initial step in an adsorption process is to select the most suitable adsorbent based on factors such as the adsorption capacity, uptake rate, production cost, and the type of adsorbate (Saleem et al., 2019). Currently, there is a significant demand for engineered nanomaterials characterized by highly porous structures and large surface area properties, as the potential candidates in heavy metal removal. Metal oxides such as iron oxide (Gusain et al., 2024), manganese oxide (Peng et al., 2015), aluminum oxide (Sen & Sarzali, 2008), zinc oxide (Sharma et al., 2019); carbon nanomaterials such as carbon nanotube (Al-Khaldi et al., 2015), graphene/graphene oxide (Bian et al., 2015), graphitic carbon nitride (Guo et al., 2018); and their combinations (Liu et al., 2016; Thy et al., 2019) have attracted considerable attention to remove Cd from aqueous systems. Metal oxides exhibit high adsorption capacities attributed to their large surface areas, high binding affinities and tunability of active surface sites (Gupta et al., 2021). However, reducing the size of metal oxides to the nanometer scale leads to a significant increase in surface energy, which compromises their stability. This instability often leads to aggregation driven by interparticular forces like Van der Waals interactions and reduces their effectiveness in adsorption processes (Hua et al., 2012). Graphene-based nanomaterials can serve as effective porous supporting materials to minimize aggregation and enhance the mechanical integrity and scalability of metal oxides. Due to the challenges and high costs associated with the large-scale synthesis of graphene-based nanomaterials, embedding them into metal oxides offers a more economically viable solution (Gupta et al., 2021; Sreeprasad et al., 2011).

Despite the extensive literature on the adsorption of Cd using metal oxide and carbon nanomaterials, there is limited research specifically focused on their combined effects. This gap in research highlights the need for further exploration into the development of hybrid material, as they possess unique properties that could improve their adsorption capacity in heavy metal removal from water systems. For example, metal oxides can be produced by cost-effective routes, regenerated through simple methods and exhibit good chemical stability across a wide range of pH levels (Kumar et al., 2013). On the other hand, graphene-based nanomaterials offer numerous active sites with an exceptional surface area and porous structure, making them particularly efficient in removing pollutants from contaminated water (Dayana Priyadharshini et al., 2022).

In this study, nickel hydroxide and graphene oxide were selected to synthesize the hybrid material due to their complementary properties and potential for enhanced adsorption performance. Nickel hydroxide is well-known for its high adsorption capacity, surface reactivity, and chemical stability, making it an effective material for removing pollutants from aqueous systems (Ogata et al., 2016; Zheng et al., 2021). As the second constituent of the composite, graphene oxide exhibits abundant oxygen-containing functional groups that facilitate the adsorption and improve the dispersion of the hybrid material. Previous studies have demonstrated the efficacy of similar hybrid materials for the removal of Cd ions from aqueous solutions (Deng et al., 2013; Wan et al., 2018).

Herein, nickel hydroxide/reduced graphene oxide [Ni(OH)$_2$/RGO] composite was synthesized via a straightforward method and employed for the efficient removal of cadmium ions from aqueous solutions. Batch adsorption experiments were systematically conducted, with key experimental parameters optimized using Response Surface Methodology (RSM) to enhance adsorption efficiency. In adsorption studies, RSM enables analysis of the influence of variables and their interactions, allowing for precise predictions of adsorption behavior. This methodology reduces the number of required experiments, thereby saving time and costs, while also identifying the most influential parameters and enhancing the understanding of process dynamics (Anfar et al., 2020). The equilibrium adsorption data obtained under optimum conditions were evaluated by fitting them to both Langmuir and Freundlich isotherm models, utilizing non-linear regression techniques to assess the adsorption behavior and model suitability.

2. EXPERIMENTAL SECTION

2.1. Chemicals and Reagents
All reagents used were of analytical grade, and ultrapure water from a Healforce Smart Mini system was used to prepare all samples and standard solutions. A Cd(II) stock solution (1000 mg/L) was obtained from High Purity Standards (North Charleston, USA), and daily working and calibration solutions were freshly diluted from the stock solution. Nickel nitrate [Ni(NO₃)₂], ammonium fluoride (NH₄F), and ammonium hydroxide (NH₄OH), essential for synthesizing Ni(OH)₂ nanoflowers, and other reagents used in synthesis of graphene oxide such as hydrogen peroxide, 35% hydrochloric acid, 95-98% sulfuric acid, 85% orthophosphoric acid, hydrazine hydrate, potassium permanganate were all purchased from Merck (Darmstadt, Germany). Nitric acid (65% v/v), purchased from Isolab (Germany), and used as the eluent. Buffer solutions at pH 4 and 6 were prepared using potassium dihydrogen phthalate (Merck, Germany), while the pH 8 buffer solution was prepared using sodium tetraborate decahydrate (Merck, Germany). Graphite powder with a high purity of 99.9995% was supplied from Alfa Aesar.

2.1. Synthesis Procedure
The synthesis of Ni(OH)₂/RGO composites followed a procedure adapted from the literature, employing a homogeneous precipitation technique (Cheng et al., 2010). Initially, graphene oxide (GO) was synthesized from graphite powder using Improved Hummer's method (Marcano et al., 2010). For the synthesis of Ni(OH)₂/RGO composites, 100 mg of GO was dispersed in 250 mL of deionized water through ultrasonication for 1.0 h. The homogeneous dispersion of GO was then added to the nickel precursor solution, which was prepared by dissolving 3.5 g of Ni(NO₃)₂ and 1.5 g of NH₄F in 250 mL of deionized water. Ammonium hydroxide solution was then added dropwise to the mixture until the pH was adjusted to 8.0. Following this, 100 µL of hydrazine hydrate was introduced to the mixture for the in-situ reduction of graphene oxide. The resulting solution was heated to 60 °C and stirred continuously for 40 minutes. Afterward, the mixture was filtered, and the particles were thoroughly washed with water and ethanol. Finally, the product was dried in an oven at 55 °C for 24 hours.

2.2. Instrumentation
The concentration of Cd in aqueous solutions was determined using a ATI UNICAM 929 AA model Flame Atomic Absorption Spectrophotometer (FAAS). The hollow cathode lamb of cadmium (Varian, USA) was operated with a wavelength of 228.2 nm, 0.50 nm spectral bandpass and 12.0 mA. A deuterium lamp was used for the correction of background. The Raman spectrum of Ni(OH)₂/RGO composite was recorded using an inVia Renishaw Raman spectrometer with a 532 nm laser beam. SEM images were captured with a FEI Quanta 600 scanning electron microscope (SEM). Prior to imaging, the nanoparticle surfaces were coated with gold-palladium using a Quorum SC7620 Sputter Coater under argon plasma.

2.2. Batch Study
Adsorption experiments were conducted in 10.0 mL of aqueous solution containing different concentrations of Cd (II). 1.0 mL of pH 8.0 buffer and 60.0 mg of Ni(OH)₂/RGO composite were added to the Cd containing solutions. The solutions were agitated on an orbital shaker for at room temperature. After 40.0 minutes, individual flasks were removed and the upper phase transferred to conical tubes for centrifugation at 5000 rpm for 5 minutes. Finally, the solutions were sent to FAAS for the determination of Cd(II) concentration. The following equations (Eq. 1 and 2) were used to calculate the removal and adsorption rates of Cd(II).

$$Q = \frac{(C_0 - C_i)xV}{m} \qquad \text{(Eq. 1)}$$

$$\%RE = \frac{(C_0 - C_i)x100}{C_0} \qquad \text{(Eq. 2)}$$

where Q refers to the adsorption capacity of composite material in mg/g, %RE is the removal percentage of Cd(II) ions, V is the solution volume in L, m is the adsorbent amount in g, C_i and C_0 are the Cd(II) concentration at final and initial stage in mg/L.

2.3. Response Surface Methodology
Box-Behnken design, as part of Response Surface Methodology (RSM), was applied to determine the optimum conditions for the adsorption process. The experimental setup involved three factors: Adsorbent dosage (A), pH (B) and mixing period (C), each evaluated at three levels (-1, 0, 1), as detailed in Table 1. A quadratic polynomial equation was used to model the experimental data, and the corresponding regression coefficients were calculated. The general form of non-linear quadratic equation is described in Equation 3 (Dean et al., 2017).

$$Y = \beta_0 + \sum_{i=1}^{n} \beta_i x_i + \sum_{i=1}^{n} \beta_{ii} x_i^2 + \sum_{i=1}^{n} \sum_{j=1}^{n} \beta_{ij} x_i x_j + \varepsilon$$
$$\text{(Eq. 3)}$$

where the term β_0 denotes to the model coefficient while $\beta_i, \beta_{ii}, \beta_{ij}$ correspond to the

linear, quadratic, and interaction coefficients, respectively. The variables x_i and x_j are the independent factors in their coded levels, n is the number of independent variables, and ε is the model error. The dependent variable represents the removal percentage of Cd(II) ion. The ranges of values for the factors in the experimental design were determined based on preliminary experiments and practical considerations relevant to the adsorption process.

Table 1: The values of variables in experimental design.

Std	Run	Factor 1 A:Adsorbent dosage, mg	Factor 2 B:pH	Factor 3 C:Mixing period, min
11	1	40	4.0	40
13	2	40	6.0	21
5	3	5.0	6.0	2.0
12	4	40	8.0	40
16	5	40	6.0	21
8	6	75	6.0	40
10	7	40	8.0	2.0
6	8	75	6.0	2.0
4	9	75	8.0	21
14	10	40	6.0	21
17	11	40	6.0	21
7	12	5.0	6.0	40
3	13	5.0	8.0	21
1	14	5.0	4.0	21
9	15	40	4.0	2.0
2	16	75	4.0	21
15	17	40	6.0	21

2.4. Adsorption Isotherm Models

Langmuir and Freundlich models were used to analyze the adsorption equilibrium data. The model equations of Langmuir and Freundlich in their non-linear forms are described in Equation 4 and 5, respectively (Al-Ghouti & Da'ana, 2020).

$$Q_e = \frac{b Q_m C_e}{1 + b C_e} \qquad \text{(Eq. 4)}$$

$$Q_e = K C_e^n \qquad \text{(Eq. 5)}$$

In Equation 4, C_e is the equilibrium concentration of Cd(II) in mg/L, while Q_e is the adsorbed amount of Cd(II) in mg/g. The maximum adsorption capacity of adsorbent and the adsorption energy are denoted by Q_m (mg/g) and b (L/mg), respectively. In Equation 5, K (mg/g (L/mg)$^{1/n}$) and n (dimensionless) are the Freundlich constants. Here, n indicates how well the adsorption process conforms to the model, while K represents the amount of Cd(II) adsorbed per unit equilibrium concentration on the adsorbent material.

In the non-linear approach, error analysis was performed using Solver add-in function in Microsoft Excel. The error function, the sum of the square of the errors (ERRSQ), was minimized to achieve the best fit between the experimental data and the estimated model predictions. The ERRSQ equation is presented as follows (Suwannahong et al., 2021):

$$ERRSQ = \sum_{i=1}^{n} \left(Q_{e,experimental} - Q_{e,predicted} \right)^2$$

(Eq. 6)

The coefficient of determination (R^2) was investigated as an indicator of model suitability. The value of R^2 ranges from 0 to 1, with higher values indicating a better model fit. The formula for R^2 as follows (Suwannahong et al., 2021):

$$R^2 = 1 - \frac{\sum_{i=1}^{n} \left(Q_{e,experimental} - Q_{e,predicted} \right)^2}{\sum_{i=1}^{n} \left(Q_{e,experimental} - \overline{Q_{e,experimental}} \right)^2}$$

(Eq. 7)

3. RESULTS AND DISCUSSION

3.1. Characterization

The morphological characterization of the $Ni(OH)_2$/RGO composite was examined using SEM analysis. The SEM image of the composite, shown in Figure 1, revealed cube-like structures of $Ni(OH)_2$ randomly distributed across the RGO sheets (Vivek et al., 2023). The FTIR spectrum of composite is displayed in Figure 2. The sharp peak at 3625 cm^{-1} was attributed to the O-H stretching vibrations, confirming the O-H bonds in beta nickel hydroxide and the presence of water molecules adsorbed between layers (Akhtar et al., 2024). The weak bands around 2900 cm^{-1} and 1048 cm^{-1} were associated with the asymmetric and symmetric CH_2 stretching and C-O-C stretching vibrations, respectively, corresponding to the remaining oxygen-containing functionalities in GO structure after reduction (Emiru & Ayele, 2017). Additionally, the characteristic band centered at 556 cm^{1} was assigned to the stretching vibrations of Ni–OH (Şaylan et al., 2022). These findings confirm the incorporation of RGO into the nickel hydroxide lattice.
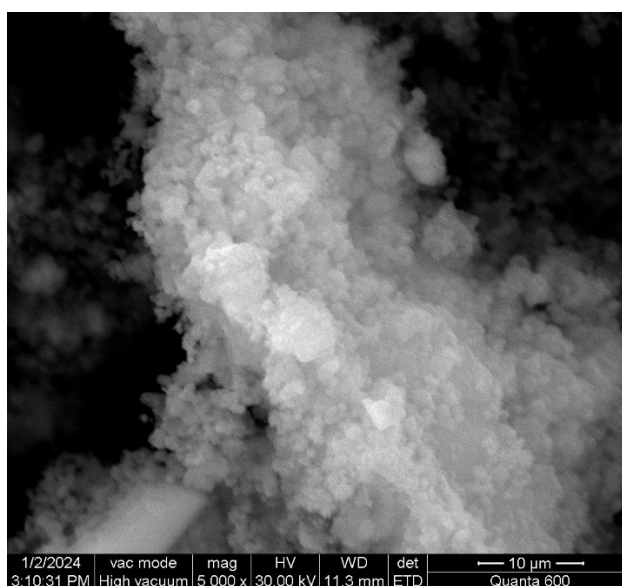

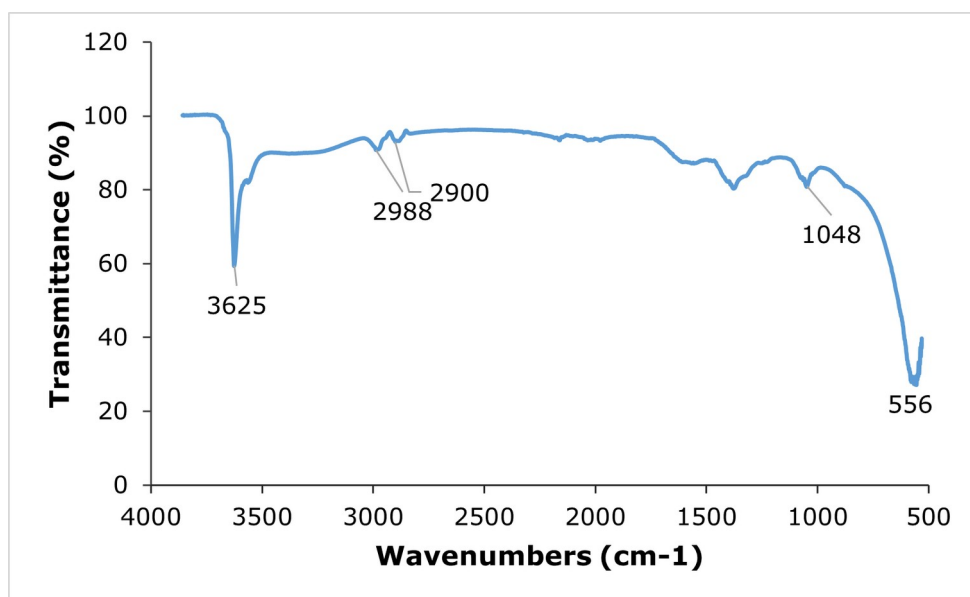**Figure 1:** SEM image of $Ni(OH)_2$/RGO composite.

Figure 2: FTIR spectrum of $Ni(OH)_2$/RGO composite.

3.2. Analytical Parameters of Cd(II) Determination

The analytical parameters of Cd(II) determination was evaluated through the limit of detection (LOD), limit of quantification (LOQ), repeatability (percent relative standard deviation, %RSD), linear range and regression analysis. The different concentrations of Cd(II) (0.10-10.0 mg/L) were prepared from the stock solution by diluting with ultrapure water. This calibration standards were analyzed by FAAS and the lowest concentration with a signal/noise ratio equal or greater than 3 was used to determine LOD and LOQ values for Cd(II)

determination. The following equations (Eq. 8 and 9) were used to LOD and LOQ values.

$$LOD = 3\,xS/m \qquad \text{(Eq. 8)}$$

$$LOQ = 10\,xS/m \qquad \text{(Eq. 9)}$$

where S is the standard deviation of at least five replicate analyses of lowest concentration and m is the slope of calibration plot constructed in the linear range. The linear range was determined as the range with a $R^2 \geq 0.99$. The analytical parameters of Cd(II) determination is given in Table 2.

Table 2: The analytical parameters of Cd(II) determination by FAAS.

Parameter	Value
LOD, mg/L	0.021
LOQ, mg/L	0.072
%RSD	6.5
Linear range, mg/L	0.10 – 5.0
R^2	0.9919

The method demonstrated LOD and LOQ values of 0.021 mg/L and 0.072 mg/L, respectively. Satisfactory repeatability was achieved, with an %RSD of 6.5% at the lowest concentration level. The linear range was established between 0.10 and 5.0 mg/L, with an R^2 value of 0.9919. Effluent and influent concentrations during the adsorption process were determined using the linear equation from the calibration plot (y = 0.0685x + 0.01). Samples with concentrations exceeding the linear range were appropriately diluted before analysis.

3.3. RSM Modelling

The experimental design for the optimization of operating conditions in the batch adsorption process was developed using Box-Behnken design. The effects of independent variables [adsorbent dosage (A), pH (B) and mixing period (C)] on the removal percentage of Cd(II) from aqueous solutions were investigated based on the analysis of variance (ANOVA). Table 3 represents the ANOVA results of experimental design.

Table 3: Analysis of variance for the experimental design of adsorptive removal of Cd(II).

Source	Sum of	df	Mean	F-value	p-value	
Model	7173	6	1195	52.1	5.7E-07	significant
A-Adsorbent dosage	2033	1	2033	88.6	2.76E-06	
B-pH	4221	1	4221	184	9.17E-08	
C-Mixing period	257	1	257	11.21	0.0074	
AB	202	1	202	8.81	0.0141	
AC	127	1	127	5.51	0.0408	
B^2	333	1	333	14.53	0.0034	
Residual	229	10	22.9			
Lack of Fit	189	6	31.4	3.08	0.1477	not significant
Pure Error	40.8	4	10.2			
Cor Total	7402	16				
R^2	0.9690					
Adjusted R^2	0.9504					
Predicted R^2	0.8619					
Adeq Precision	25.32					

The results given in Table 3 demonstrated a strong model fit, with a highly significant p-value (p < 0.0001) and an insignificant lack of fit. This indicated that the chosen variables were well-suited for the model, accurately representing the experimental data and confirming its reliability for predicting response values. The robustness of the model was further validated by a high R^2 value of 0.9690, which was close to 1.00, indicating a good fit to the experimental data and strong predictive power. In addition to that, the satisfactory alignment between the predicted R^2 (0.9504) and adjusted R^2 (0.8619) showed the reliability of model, confirming the minimal overfitting and consistent performance in predicting and adjusting the datasets (Roy et al., 2014).

The independent variables, adsorbent dosage, pH and mixing period, were found to be significant factors in the adsorption process. Significant interaction effects were observed between adsorbent dosage and pH, as well as adsorbent dosage and mixing period, indicating that these variables influence each other's effect on adsorption efficiency. Furthermore, the quadratic term for pH revealed a non-linear relationship, showing the importance of optimizing pH for maximum adsorption. The response surface graphs showing the removal percentage as a function of the interactions between the two variables are illustrated in Figure 3. In this analysis, the two parameters were varied while the other was held constant.
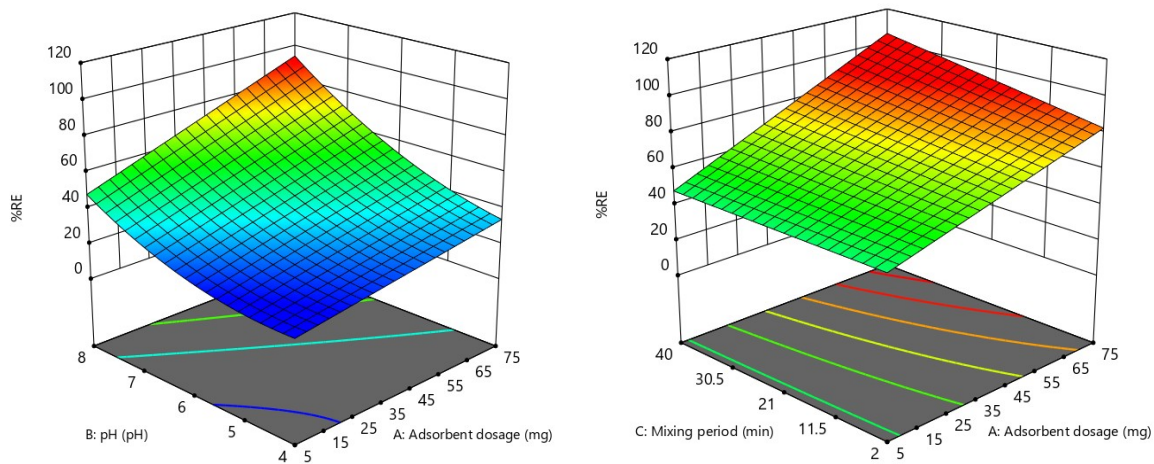

Figure 3: 3D response surface plots for Cd(II) removal percentage for the interaction between two operating parameters.

As seen in Figure 3, the removal percentage of Cd(II) increased with the increase in adsorbent dosage, likely due to the increase in the presence of active sites. pH was identified as the most influential factor in the removal of Cd(II) ions. The removal efficiency increased significantly, from 20% to 91%, as the pH of solution was increased from 4 to 8. This improvement was attributed to the formation of favorable conditions for electrostatic attraction between the negatively charged adsorbent surface and positively charged Cd(II) ions at higher pH levels (Lin et al., 2018). The highest cadmium removal was observed at pH 8. To assess the potential for Cd(II) ion precipitation as hydroxides, control experiments were conducted with Cd(II) spiked samples at a fixed

concentration, without the addition of adsorbent. The absorbance values of Cd(II) solution in ultrapure water were compared with those at pH 8.0, and the reduction in absorbance was used as an indicator of Cd(II) precipitation. Results showed that only about 12% of Cd(II) was converted into hydroxides, suggesting that the conditions did not lead to significant precipitation. This finding supports the conclusion that adsorption, rather than precipitation, was the primary removal mechanism for Cd(II) in this study.

The quadratic model used to predict the removal percentage (%RE) of Cd(II) from aqueous solutions using Ni(OH)$_2$/RGO composite is expressed in Equation 10.

$$\%RE = 57.2362 - 0.3315\,A - 19.1913\,B - 0.03979\,C + 0.101557\,AB + 0.008457\,AC + 2.2178\,B^2$$
(10)

As a result, the optimum conditions of the batch adsorption process were determined to be an 60 mg of adsorbent dosage, pH 8.0 and a

mixing period of 40 minutes. The average removal percentage of Cd(II) under optimum conditions was calculated as %93.

3.4. Isotherm analysis by nonlinear regression

A nonlinear approach was applied to analyze the adsorption data using Langmuir and Freundlich isotherm models. Error analyses were performed to estimate isotherm parameters with ERRSQ employed as the error function to be minimized. The estimated parameters of adsorption isotherms are presented in Table 4.

Table 4: The isotherm parameters of Langmuir and Freundlich models estimated by nonlinear regression.

	Parameter	Value
Langmuir	Q_m (mg/g)	218.12
	b (L/mg)	0.2418
	R^2	0.9684
	ERRSQ	132.8
Freundlich	K (mg/g) (L/mg)$^{1/n}$	40.83
	n	0.775
	R^2	0.9487
	ERRSQ	215.9

As given in Table 4, the adsorption data analysis indicated that the Langmuir model provided a better fit than the Freundlich model for Cd(II) adsorption. The maximum adsorption capacity (Q_m) was found to be 218.12 mg/g, suggesting a high adsorption potential, while the Langmuir constant (b) indicated moderate affinity between the adsorbent and adsorbate ions (Al-Ghouti & Da'ana, 2020). A high correlation coefficient (R^2=0.9684) and lower error sum of squares (ERRSQ=132.8) further confirmed the suitability of the Langmuir model, suggesting monolayer adsorption on a homogeneous surface (Ncibi, 2008). In comparison, the lower R^2 and higher ERRSQ for Freundlich revealed that it was less effective in representing the adsorption behavior accurately.

The performance of the synthesized hybrid material was compared with similar adsorbents reported in the literature, particularly graphene oxide/metal oxide nanocomposites for Cd removal. For example, magnetic graphene oxide demonstrated a maximum adsorption capacity of 91.29 mg/g (Deng et al., 2013), while reduced graphene oxide-zinc oxide nanocomposites achieved 49.99 mg/g for the removal of Cd(II) from contaminated wastewater (Motitswe et al., 2024). Similarly, magnetic iron oxide/graphene oxide (Fe_3O_4/GO) nanocomposites exhibited a maximum adsorption capacity of 52.083 mg/g for Cd(II) removal (Thy et al., 2019). Furthermore, in another study, the maximum adsorption capacity was reported as 45.05 mg/g using a magnetic graphene oxide/MgAl-layered double hydroxide nanocomposite for cadmium in aqueous solutions during batch equilibrium experiments (Huang et al., 2018). In terms of adsorption behavior, magnetic graphene oxide (Deng et al., 2013) and magnetic iron oxide/graphene oxide nanocomposites (Thy et al., 2019) also followed the Langmuir model, with electrostatic interactions and surface functional groups playing a significant role in adsorption. In contrast, reduced graphene oxide-zinc oxide nanocomposites (Motitswe et al., 2024) exhibited a combination of heterogeneous and homogeneous coverage, with adsorption mechanisms attributed to ionic bonding and dipole–dipole interactions involving oxygen groups on ZnO nanoparticle. Huang et al. (2018) identified multiple mechanisms, including surface complexation, precipitation of metal hydroxides, and isomorphic replacement, for Cd(II) adsorption on MgAl-layered double hydroxides, while the Langmuir model was also observed (Huang et al., 2018). Overall, while diverse mechanisms and adsorption behaviors were reported across these studies, the high adsorption capacity and strong interactions observed in this study revealed the potential of the $Ni(OH)_2$/RGO composite as an effective adsorbent for Cd(II) removal from aqueous environments.

4. CONCLUSION

In this study, the adsorption of Cd(II) ions from aqueous solutions using $Ni(OH)_2$/RGO composite was investigated for the efficient removal of this element. The effects of mixing period, pH and adsorbent dosage were examined to achieve maximum adsorption efficiency. Response surface methodology using Box-Behnken design was employed to optimize the influential parameters. pH of solution and adsorbent dosage were identified as key parameters influencing Cd(II) removal. The adsorption isotherm analysis was performed using nonlinear regression analysis. The Langmuir model provided the best fit, with an R^2 value close to 1 and low value of error function. This finding suggested monolayer adsorption on a uniform surface with finite adsorption sites, indicative of a strong, specific interaction between the adsorbent and Cd(II) ions. With a high maximum adsorption capacity of 218 mg/g, the $Ni(OH)_2$/RGO composite demonstrates

considerable potential as an effective material for Cd(II) removal in aqueous environments.

5. CONFLICT OF INTEREST

The author declares that she has no known competing financial interests or personal relationships that could have appeared to influence the work reported in this paper.

6. REFERENCES

Akhtar, M. S., Wejrzanowski, T., Komorowska, G., Adamczyk-Cieślak, B., & Choinska, E. (2024). Microwave-assisted hydrothermal synthesis of αβ-Ni(OH)2 nanoflowers on nickel foam for ultra-stable electrodes of supercapacitors. Electrochimica Acta, 508, 145284. https://doi.org/https://doi.org/10.1016/j.electacta.2024.145284

Al-Ghouti, M. A., & Da'ana, D. A. (2020). Guidelines for the use and interpretation of adsorption isotherm models: A review. Journal of Hazardous Materials, 393, 122383.

Al-Khaldi, F. A., Abu-Sharkh, B., Abulkibash, A. M., & Atieh, M. A. (2015). Cadmium removal by activated carbon, carbon nanotubes, carbon nanofibers, and carbon fly ash: a comparative study. Desalination and Water Treatment, 53(5), 1417–1429.

Anfar, Z., Ait Ahsaine, H., Zbair, M., Amedlous, A., Ait El Fakir, A., Jada, A., & El Alem, N. (2020). Recent trends on numerical investigations of response surface methodology for pollutants adsorption onto activated carbon materials: A review. Critical Reviews in Environmental Science and Technology, 50(10), 1043–1084.

Bian, Y., Bian, Z.-Y., Zhang, J.-X., Ding, A.-Z., Liu, S.-L., & Wang, H. (2015). Effect of the oxygen-containing functional group of graphene oxide on the aqueous cadmium ions removal. Applied Surface Science, 329, 269–275.

Charkiewicz, A. E., Omeljaniuk, W. J., Nowak, K., Garley, M., & Nikliński, J. (2023). Cadmium Toxicity and Health Effects—A Brief Summary. In Molecules (Vol. 28, Issue 18). https://doi.org/10.3390/molecules28186620

Cheng, Z., Xu, J., Zhong, H., Li, D., Zhu, P., & Yang, Y. (2010). A facile and novel synthetic route to Ni(OH)2 nanoflowers. Superlattices and Microstructures, 48(2), 154–161. https://doi.org/https://doi.org/10.1016/j.spmi.2010.05.013

Dayana Priyadharshini, S., Manikandan, S., Kiruthiga, R., Rednam, U., Babu, P. S., Subbaiya, R., Karmegam, N., Kim, W., & Govarthanan, M. (2022). Graphene oxide-based nanomaterials for the treatment of pollutants in the aquatic environment: Recent trends and perspectives – A review. Environmental Pollution, 306, 119377. https://doi.org/https://doi.org/10.1016/j.envpol.2022.119377

Dean, A., Voss, D., Draguljić, D., Dean, A., Voss, D., & Draguljić, D. (2017). Response surface methodology. Design and Analysis of Experiments, 565–614.

Deng, J.-H., Zhang, X.-R., Zeng, G.-M., Gong, J.-L., Niu, Q.-Y., & Liang, J. (2013). Simultaneous removal of Cd(II) and ionic dyes from aqueous solution using magnetic graphene oxide nanocomposite as an adsorbent. Chemical Engineering Journal, 226, 189–200. https://doi.org/https://doi.org/10.1016/j.cej.2013.04.045

Emiru, T. F., & Ayele, D. W. (2017). Controlled synthesis, characterization and reduction of graphene oxide: A convenient method for large scale production. Egyptian Journal of Basic and Applied Sciences, 4(1), 74–79.

Goyal, P., Tiwary, C. S., & Misra, S. K. (2021). Ion exchange based approach for rapid and selective Pb (II) removal using iron oxide decorated metal organic framework hybrid. Journal of Environmental Management, 277, 111469.

Gulisano, M., Pacini, S., Punzi, T., Morucci, G., Quagliata, S., Delfino, G., Sarchielli, E., Marini, M., & Vannelli, G. B. (2009). Cadmium modulates proliferation and differentiation of human neuroblasts. Journal of Neuroscience Research, 87(1), 228–237. https://doi.org/https://doi.org/10.1002/jnr.21830

Guo, S., Wu, K., Gao, Y., Liu, L., Zhu, X., Li, X., & Zhang, F. (2018). Efficient removal of Zn (II), Pb (II), and Cd (II) in waste water based on magnetic graphitic carbon nitride materials with enhanced adsorption capacity. Journal of Chemical & Engineering Data, 63(10), 3902–3912.

Gupta, K., Joshi, P., Gusain, R., & Khatri, O. P. (2021). Recent advances in adsorptive removal of heavy metal and metalloid ions by metal oxide-based nanomaterials. Coordination Chemistry Reviews, 445, 214100. https://doi.org/https://doi.org/10.1016/j.ccr.2021.214100

Gusain, D., Sahani, S., Sharma, Y. C., & Han, S. S. (2024). Adsorption of cadmium ion from water by using non-toxic iron oxide adsorbent; experimental and statistical modelling analysis. International Journal of Environmental Science and Technology, 1–16.

Hayat, M. T., Nauman, M., Nazir, N., Ali, S., & Bangash, N. (2019). Environmental Hazards of Cadmium: Past, Present, and Future. Cadmium Toxicity and Tolerance in Plants: From Physiology to Remediation, 163–183. https://doi.org/10.1016/B978-0-12-814864-8.00007-3

Hosseini, S. M., Alibakhshi, H., Jashni, E., Parvizian, F., Shen, J. N., Taheri, M., Ebrahimi, M., & Rafiei, N. (2020). A novel layer-by-layer heterogeneous cation exchange membrane for heavy metal ions removal from water. Journal of Hazardous Materials, 381, 120884.

Hua, M., Zhang, S., Pan, B., Zhang, W., Lv, L., & Zhang, Q. (2012). Heavy metal removal from water/wastewater by nanosized metal oxides: A review. Journal of Hazardous Materials, 211–212, 317–331. https://doi.org/10.1016/j.jhazmat.2011.10.016

Huang, Q., Chen, Y., Yu, H., Yan, L., Zhang, J., Wang, B., Du, B., & Xing, L. (2018). Magnetic graphene oxide/MgAl-layered double hydroxide nanocomposite: One-pot solvothermal synthesis, adsorption performance and mechanisms for Pb2+, Cd2+, and Cu2+. Chemical Engineering Journal, 341, 1–9. https://doi.org/https://doi.org/10.1016/j.cej.2018.01.156

Kim, J. G., Ku, J., Jung, J., Park, Y. S., Choi, G. H., Hwang, S. S., Lee, J.-H., & Lee, A. S. (2024). Ion-exchangeable and sorptive reinforced membranes for efficient electrochemical removal of heavy metal ions in wastewater. Journal of Cleaner Production, 438, 140779.

Kumar, K. Y., Muralidhara, H. B., Nayaka, Y. A., Balasubramanyam, J., &

Hanumanthappa, H. (2013). Low-cost synthesis of metal oxide nanoparticles and their application in adsorption of commercial dye and heavy metal ion in aqueous solution. Powder Technology, 246, 125–136. https://doi.org/https://doi.org/10.1016/j.powtec.2013.05.017

Lin, J., Su, B., Sun, M., Chen, B., & Chen, Z. (2018). Biosynthesized iron oxide nanoparticles used for optimized removal of cadmium with response surface methodology. Science of The Total Environment, 627, 314–321. https://doi.org/https://doi.org/10.1016/j.scitotenv.2018.01.170

Liu, J., Ge, X., Ye, X., Wang, G., Zhang, H., Zhou, H., Zhang, Y., & Zhao, H. (2016). 3D graphene/δ-MnO 2 aerogels for highly efficient and reversible removal of heavy metal ions. Journal of Materials Chemistry A, 4(5), 1970–1979.

Marcano, D. C., Kosynkin, D. V., Berlin, J. M., Sinitskii, A., Sun, Z., Slesarev, A., Alemany, L. B., Lu, W., & Tour, J. M. (2010). Improved synthesis of graphene oxide. ACS Nano, 4(8), 4806–4814. https://doi.org/10.1021/nn1006368

Motitswe, M. G., Badmus, K. O., & Khotseng, L. (2024). Application of Reduced Graphene Oxide-Zinc Oxide Nanocomposite in the Removal of Pb(II) and Cd(II) Contaminated Wastewater. In Applied Nano (Vol. 5, Issue 3, pp. 162–189). https://doi.org/10.3390/applnano5030012

Ncibi, M. C. (2008). Applicability of some statistical tools to predict optimum adsorption isotherm after linear and non-linear regression analysis. Journal of Hazardous Materials, 153(1), 207–212. https://doi.org/https://doi.org/10.1016/j.jhazmat.2007.08.038

Ogata, F., Imai, D., Toda, M., Otani, M., & Kawasaki, N. (2016). Properties of a novel adsorbent produced by calcination of nickel hydroxide and its capability for phosphate ion adsorption. Journal of Industrial and Engineering Chemistry, 34, 172–179.

Peana, M., Pelucelli, A., Chasapis, C. T., Perlepes, S. P., Bekiari, V., Medici, S., & Zoroddu, M. A. (2023). Biological Effects of Human Exposure to Environmental Cadmium. In Biomolecules (Vol. 13, Issue 1). https://doi.org/10.3390/biom13010036

Peng, L., Zeng, Q., Tie, B., Lei, M., Yang, J., Luo, S., & Song, Z. (2015). Manganese dioxide nanosheet suspension: a novel absorbent for cadmium (II) contamination in waterbody. Journal of Colloid and Interface Science, 456, 108–115.

Pohl, A. (2020). Removal of heavy metal ions from water and wastewaters by sulfur-containing precipitation agents. Water, Air, & Soil Pollution, 231(10), 503.

Roy, P., Mondal, N. K., & Das, K. (2014). Modeling of the adsorptive removal of arsenic: A statistical approach. Journal of Environmental Chemical Engineering, 2(1), 585–597. https://doi.org/https://doi.org/10.1016/j.jece.2013.10.014

Saleem, J., Shahid, U. Bin, Hijab, M., Mackey, H., & McKay, G. (2019). Production and applications of activated carbons as adsorbents from olive stones. Biomass Conversion and Biorefinery, 9(4), 775–802. https://doi.org/10.1007/s13399-019-00473-7

Şaylan, M., Demirel, R., Ayyıldız, M. F., Chormey, D. S., Çetin, G., & Bakırdere, S. (2022). Nickel hydroxide nanoflower–based dispersive solid-phase extraction of copper from water matrix. Environmental Monitoring and Assessment, 195(1), 133. https://doi.org/10.1007/s10661-022-10653-0

Sen, T. K., & Sarzali, M. V. (2008). Removal of cadmium metal ion (Cd2+) from its aqueous solution by aluminium oxide (Al2O3): A kinetic and equilibrium study. Chemical Engineering Journal, 142(3), 256–262.

Sharma, M., Singh, J., Hazra, S., & Basu, S. (2019). Adsorption of heavy metal ions by mesoporous ZnO and TiO2@ZnO monoliths: Adsorption and kinetic studies. Microchemical Journal, 145, 105–112. https://doi.org/https://doi.org/10.1016/j.microc.2018.10.026

Sreeprasad, T. S., Maliyekkal, S. M., Lisha, K. P., & Pradeep, T. (2011). Reduced graphene oxide–metal/metal oxide composites: Facile synthesis and application in water purification. Journal of Hazardous Materials, 186(1), 921–931. https://doi.org/https://doi.org/10.1016/j.jhazmat.2010.11.100

Sun, J., Liu, L., & Yang, F. (2020). A WO3/PPy/ACF modified electrode in electrochemical system for simultaneous removal of heavy metal ion Cu2+ and organic acid. Journal of Hazardous Materials, 394, 122534.

Suwannahong, K., Wongcharee, S., Kreetachart, T., Sirilamduan, C., Rioyo, J., & Wongphat, A. (2021). Evaluation of the Microsoft Excel Solver Spreadsheet-Based Program for nonlinear expressions of adsorption Isotherm models onto magnetic nanosorbent. Applied Sciences, 11(16), 7432.

Thy, L. T. M., Thuong, N. H., Tu, T. H., Nam, H. M., Hieu, N. H., & Phong, M. T. (2019). Synthesis of magnetic iron oxide/graphene oxide nanocomposites for removal of cadmium ions from water. Advances in Natural Sciences: Nanoscience and Nanotechnology, 10(2), 25006.

Vivek, P., Sivakumar, R., Selva Esakki, E., & Deivanayaki, S. (2023). Fabrication of NiO/RGO nanocomposite for enhancing photocatalytic performance through degradation of RhB. Journal of Physics and Chemistry of Solids, 176, 111255. https://doi.org/https://doi.org/10.1016/j.jpcs.2023.111255

Wan, S., Ding, W., Wang, Y., Wu, J., Gu, Y., & He, F. (2018). Manganese oxide nanoparticles impregnated graphene oxide aggregates for cadmium and copper remediation. Chemical Engineering Journal, 350, 1135–1143.

Zhang, Y., & Duan, X. (2020). Chemical precipitation of heavy metals from wastewater by using the synthetical magnesium hydroxy carbonate. Water Science and Technology, 81(6), 1130–1136.

Zheng, Y., Cheng, B., Fan, J., Yu, J., & Ho, W. (2021). Review on nickel-based adsorption materials for Congo red. Journal of Hazardous Materials, 403, 123559.